Development, Analyze and Preclinical Evaluation of Inactivated Vaccine Candidate For Prevention of COVID-19 Disease

Engin Alp Onen (alponen@gmail.com)
VTI Laboratories https://orcid.org/0000-0003-1661-5803
Kivilcim SONMEZ
Istanbul Universitesi Veteriner Fakultesi
Funda YILDIRIM
Istanbul Universitesi Veteriner Fakultesi
Elif kervancioglu DEMİRCİ
Istanbul Universitesi Istanbul Tip Fakultesi
Aydin GUREL
Istanbul Universitesi Veteriner Fakultesi

Research

Keywords: SARS-CoV-2, Beta-coronaviruses, virology, inactivated vaccines, micro neutralization test, TEM analysis, VERO cells, histopathology, preclinical trials

Posted Date: October 19th, 2021

DOI: https://doi.org/10.21203/rs.3.rs-960262/v1

Abstract

Background

A novel coronavirus, severe acute respiratory syndrome coronavirus 2 (SARS-CoV-2), emerged in the Chinese capital Wuhan in 2019. Since late 2019, SARS-CoV-2 has been responsible for a global pandemic that has resulted in 205,338,159 confirmed cases of infection and 4,333,094 deaths as of August 11, 2021, according to the World Health Organization. Currently, there are no approved antiviral drugs and vaccines against SARS-CoV-2. Several strategies to develop SARS-CoV-2 vaccines rely on different technologies such as DNA- and RNA-based formulations, recombinant subunits with viral particles, viral vectors, and purified inactivated viral formulations with or without adjuvant.

Method

Here we report the development of an inactivated SARS-CoV-2 vaccine candidate and show that its efficacy and safety in preclinical studies warrant further clinical evaluation. For this purpose, a vaccine candidate was manufactured by using microcarrier based cell culture methods in a disposable wave bioreactor, purified by using ultrafiltration and multimodal chromatography system, and their effect and possible side effects on different doses were evaluated using qRT-PCR, Western Blotting, antigen ELISA, histopathology, serum neutralization test in Balb/c mice.

Results

Microcarrier-based production in disposable wave bioreactors (SARTORIUS Biostat RM20, Germany) was very efficient for vaccine production. Each dose of the vaccine candidate contains about 340 –400 ng viral spike protein. TEM analysis verified the viral replication in VERO cells and showed intact, oval-shaped particles with diameters of 90 to 110 nm of the virus after the final purification step. The preliminary results in mice showed that the NtAb titers reached the peak post-priming and boosting in 21 days. The titers were respectively 1/ 595, 1 /791, and 1/1048 in 4, 6, and 10 µg groups. In transgenic ferrets, the inactivated vaccine doses were well tolerated in all dose groups with no vaccine-related serious adverse effects.

Conclusions

In conclusion, two different doses (4 and 6 micrograms) of the inactivated SARS-CoV-2 candidate vaccine administered twice were shown to be effective and safe in preclinical studies. All analytical studies have shown that the quality control parameters of the vaccine candidate meet the requirements for inactivated viral vaccines.

Introduction

The new coronavirus SARS-CoV-2, the causative agent of 2019 coronavirus disease (COVID -19), belongs to the genus Beta coronaviruses. This genus also includes SARS-CoV and MERS-CoV (Qiang Gao, Linlin Bao, Haiyan Mao 2020). SARS-CoV-2 is closely related to severe acute respiratory syndrome coronavirus (SARS-CoV) and several bat coronaviruses. SARS-CoV-2 has a linear single-stranded positive-sense RNA genome of 30 kb in length encoding four structural proteins (spike (S), envelope (E), membrane (M), and nucleocapsid (N)), sixteen non-structural proteins, and several accessory proteins. Spike (S) is the binding domain and a major structural protein that elicits highly potent neutralizing antibodies (NAbs). SARS-CoV-2 binds to ACE2 receptors via the RBD (Receptor Binding Domain) of the spike protein to initiate membrane fusion and enter human cells. Some critical amino acid residues (AA) in the RBD were different between SARS-CoV-2 and SARS-CoV [1–4].

Neutralizing antibodies (NAbs) are key components of the protective immune response to viral infections, as they can bind to and block viral particles and help to serve APC (antigen-presenting cells [5–7].

Methods

A SARS-CoV-2 strain isolated from bronchoalveolar lavage specimens or throat swabs from a hospitalized patient in the recent COVID -19 outbreak by the Turkish Ministry of Health was used to develop a candidate vaccine. This strain was isolated from VERO cells, which are approved by WHO as a cell line to produce inactivated vaccines for human use. This primary seed was further amplified to create a master seed virus bank, a working virus bank, and a production virus bank.

Highly efficient propagation and high genetic stability are key characteristics for the development of an inactivated vaccine. It was found that the strain showed optimal replication and generated high virus yields on Green Monkey Kidney Cells (VERO CCL-81, ATCC) were cultured in Eagle's modified Essential medium (EMEM) (Sigma, Germany) supplemented with 10% heat-inactivated fetal bovine serum (FBS) (Sigma, Germany) and L-glutamine. In the present study, the strain showed optimal replication and produced high virus yields. Here, we set out to determine the most appropriate times post-infection to harvest. We determined that the cytopathic effect (CPE) caused by SARS-CoV-2 in Vero cells is most apparent at 48 h post-infection (Figure 1B). The highest CPE is at 62 h post-infection (Figure 1C).

Initially, CCL-81 Vero cells were seeded in T-flasks (NEST, USA) at 2.105 /cm^2 and incubated in a humidified incubator at 37 °C with 5% CO_2 (Figure 2A). Four days after seeding, confluent cells were trypsinized at a ratio of 0.25% trypsin-EDTA and transferred to the 3.165 cm^2 BioFactory Chamber 5 (NEST, USA). In addition, two T-175 flasks were infected with SARS-CoV-2 virus seed lots to produce a bioreactor inoculum (Figure 2B). Four days after the cells were seeded in the BioFacoty chamber, they were passaged onto a microcarrier system (3 to 5 mg/L Cytodex-1, GE, USA) in a 20-liter bioreactor (Figure 2C). Vero cells were cultured in a 20-liter bioreactor at a temperature of 37 ± 1°C. The pH of 7.2 was regulated by CO2 and the addition of NaHCO3 at 88 g/L, and dissolved oxygen was adjusted to 35-98% air saturation by continuous surface aeration. To produce the SARS-CoV-2 virus, the virus seeds were inoculated at a ratio of 0.05 MOI

after washing the cells with DPBS (Sigma Aldrich, USA) solution, the pH was maintained at 6.8 - 7.1, the pO2 at 35 – 98 % air saturation, and the temperature at 37°C. The rotation speed was 12 - 18 rpm and the angle was 6°-7° depends on the different cell growing and viral incubation stages. Growth kinetic analysis of the P5 strain in Vero cells showed that the strain virus could replicate efficiently and reached a peak titer of 1.6 x 10^7 PFU after 56 - 72 hours at infection multiplicities (MOI) of 0.01-0.05 [6]. The virus mass was harvested at 62 h (Figure 2D) after inoculation and then inactivated with β-propiolactone at a validated ratio at 2 - 6°C for 16 - 20 h, followed by benzonase-endonuclease treatment at room temperature, concentration by ultrafiltration, and multimodal chromatographic purification. During the inactivation process, the pH was maintained at 6.8-7.1. The final mass was prepared by adding 0.05% (v/v) Alhydrogel (Croda, Denmark) as adjuvant and dilution buffer containing Phosphate Buffer Saline (PBS, Sigma Aldrich) with stirring at 20 - 30 rpm at 25 °C for 2 hours [8].

Since safety and efficiency are critical for vaccine development, all sterility, Mycoplasma sp. and endotoxin analyzes were performed according to European Pharmacopeia and acceptable levels were found. However, Vero Cell Banks and Virus Seed Lots were found to be free of mycoplasma by culture and isolation method according to Pharmacopeia.

In the present study, a purified inactivated SARS-CoV-2 virus vaccine candidate was prepared at a pilot scale to induce specific neutralizing antibodies in 6 – 8 weeks old Balb/c mice. Five immunization doses (10 µg, 6 µg, 4 µg, 1 µg per dose and placebo) mixed with 0.05 % (v/v) Alhydrogel adjuvant were administered to five groups of mice (n=10). Partial and complete protection against challenge by observing an increase in serum neutralizing antibody levels, pneumonia symptoms, and histopathological examination of the lungs [5,6].

Virus titration and vaccine preparation

SARS-CoV-2 viral titer was determined using a plaque assay. Serial 10-fold dilutions of virus-containing samples were inoculated into 12-well culture plates seeded with confluent Vero cells. 1 hour later, the inoculums were removed and then covered with 0.4% agarose MEM. After 3 days of culture in a 5% CO2 incubator at 37 °C, the cells were fixed with 10% neutralized formalin for 1 hour at room temperature. After the fixation process, the agarose layer was removed with pipette tips and crystal violet solution (0.4%) was added to the wells. After the washing process, the wells were checked for plaque formation and the titer was calculated as Plaque Forming Unit (PFU/ml)

PFU/ml = Average Plaques Number / Dilution factor x Volume of diluted virus added to the well
PFU/ml = 8 / 10^{-6} x 0,5
PFU/ml = 1.6 x 10^7

Validation of inactivation

3 ml of the inactivated SARS-CoV-2 was used to inoculate Vero cell monolayers in 25 cm2 flasks, and negative control cells were prepared; the cells were then cultured at 36 ± 1 °C for 4 days. Then, 5 ml supernatant of cells in the flask was inoculated onto two more Vero cell monolayers in 25 cm^2 flasks (5 ml each) and incubated at 36 ± 1 °C for 4 days. This was the second passage. Then 5 ml supernatant of cells from the flask was inoculated onto more Vero monolayers in 75 cm^2 flasks and incubated for 4 days at 36 ± 1 °C. This was the third passage. No CPE was observed in three passages [8]. Inactivation was validated by passaging the treated samples for 3 (n=3) generations without CPE occurring.

Immunogenicity analysis of the vaccine and neutralization assay.

An ideal serological assay should measure the binding of neutralizing antibodies to the SARS-CoV-2 spike protein. For this purpose, Balb/c mice were randomly divided into five groups (10 animals in each group) and intraperitoneally (IP) injected with the experimental vaccine at five different doses (0 µg, 1 µg, 4 µg, 6 µg and 10 µg per dose, mixed with alum adjuvant) on the 0th and 21st [7], blood was collected from the mice at 0, 7, 14, 21 and 35 days after immunization. Each animal was injected intraperitoneally with 0.2 ml of the test sample (equivalent to one human dose).

Serum from the mice to be tested was diluted 1:2 in advance and inactivated in a 56°C water bath for 30 minutes. The serum was diluted 1:2 by a 2-fold dilution series to the required concentration, and an equal volume of a challenge virus solution containing 100 $CCID_{50}$ viruses was added. After neutralization in a 37°C incubator for 1 hour, a 1 x 10^6/ml cell suspension was added to the wells (0.1 ml/well) and cultured in a CO_2 incubator at 37°C for 4 days. The CPE observation was used to calculate the neutralization endpoint (conversion of serum dilution to logarithm) according to the Karber method [9], i.e., the highest serum dilution that can protect 50% of the cells from infection by 100 $CCID_{50}$ viruses is the antibody potency of the serum. A neutralization antibody potency of 1:4 is negative, while one of 1:4 is positive [10–12].

Transmission Electron Microscopy (TEM) sample preparation

Inactivated samples and infected Vero cells were mounted on pyeloform-coated nickel grids, stained with 2% uranyl acetate, washed with sterile pure water, and visualized in a transmission electron microscope (Jeol, Tokyo, Japan) [8]. A specialized histologist and a virologist made the observations.

Nucleic acid extraction and first-strand cDNA synthesis

We extracted total nucleic acid from 200 µL of clarified viral supernatants using the Mini Pathogen Nucleic Acid Kit (QIAGEN) according to the manufacturer's instructions and collected 50 µL elution volumes. The viral RNA was reverse transcribed using the Moloney murine leukemia virus reverse transcriptase (M-

MLV RT) (Thermo Scientific, USA) using random hexamers according to the manufacturer's recommendations. The reaction mixtures were incubated for 60 min at 42˚C, and the reaction was stopped by heating the mixture at 95˚C for 5 min and chilling it on ice.

Sequencing

For whole-genome sequencing of SARS-CoV-2 samples, Quant-it RNA HS Assay kit (Invitrogen, USA) and Qubit fluorometer were used for measurement of isolated RNA samples. Library preparation was performed using the CleanPlex® SARS-CoV-2 Panel (Paragon Genomics) with isolated RNA samples following the kit's recommended instructions. Libraries were sequenced on the Illumina NextSeq (Illumina, USA) platform with a 2x150 loop kit with an average of 500,000 reads. The quality of raw data was examined with FastQC v.0.11.5 and low-quality bases and primers were trimmed using Trimmomatic v.0.32. Reads were aligned to the known SARS-CoV-2 genome (GenBank Access: MN908947.3) using the Burrows-Wheeler aligner v.0.7.1. Variants were detected using the Genome Analysis Toolkit -HaplotypeCaller (GATK) v.3.8.0 and analyzed on GenomeBrowse v2.1.2 (GoldenHelix). The genome sequences of the first viral sample obtained and the genome sequence of the last sample was aligned using BLAST+ [13].

Quantitative Real-Time PCR

rRT-PCR assay rRT-PCR assay was performed using the One-Step RT -qPCR Master Mix, (Genesig/primer design, USA). Each 20-µL reaction contained 10 µL 2X Master Mix (Genesig/primer design, USA), 1.5 µL 5 µmol/L probes, 20 µmol/L forward and reverse primer mix, 3.5 µL nuclease-free water, and 5 µL nucleic acid extract. We performed amplification in 96-well plates on a ROCHE Light Cycler 480 Real-Time PCR instrument (ROCHE). Real-time PCR conditions RT consisted of 10 min at 55°C for reverse transcription, 2 min at 95°C for Taq enzyme activation, and 40 cycles of 3 s at 95°C and 30 s at 55°C. A positive test result was defined as an exponential fluorescence curve that exceeded the threshold within 40 cycles at the FAM channel [14].

SDS- PAGE and WESTERN BLOTTING

Beta-propiolactone inactivated SARS-CoV-2 virus samples were separated using the 10% polyacrylamide gels described by Laemmli and visualized using the Commosie Blue staining kit (BIO-RAD). Another SDS -PAGE (Bio-Rad TGX Mini, Bio-Rad, Hercules, CA, USA) gel was transferred to a 0.2 µM PVDF membrane according to the manufacturer's protocols (Bio-Rad Transblot Turbo; Bio-Rad, Hercules, CA, USA). After blocking with 5% non-fat dry milk in TBST (10 mM Tris, 150 mM NaCl, 0.5% Tween-20, pH8) for one hour, the membranes were incubated overnight at 4 °C with antibodies against SARS-CoV N (Sino Biological, Wayne, PA, USA; 40588-T62) and SARS-CoV S (Sino Biological, Wayne, PA, USA; 40589-T62). Membranes were washed in TBST and incubated with an HRP-conjugated rabbit secondary antibody (Cell Signaling, Danvers, MA, USA; 7074) for 1 hour at room temperature. Membranes were then washed, developed with ECL, and imaged on a Bio-Rad Chemidoc imaging system. The molecular weights of the full-length S, N, and M proteins are approximately 190, 48, and 26 kDa, respectively.

SARS-CoV-2 Spike Protein Quantitation detection by sandwich ELISA method.

SARS-CoV-2 Spike Protein was quantified by sandwich ELISA using the SARS-CoV-2 (2019-nCoV) Spike Protein ELISA kit (Creative Biolabs, Life Technology, NY, USA) according to the manufacturer's instructions. The SARS-CoV-2 (2019-nCoV) Spike Protein ELISA kit is based on a solid-phase sandwich enzyme immunoassay. The wells of the plate strips are coated with a monoclonal antibody specific for SARS-CoV-2 spike protein and nucleoprotein. Since the 10000 pg/ml standard serves as a high standard, we diluted the samples hundreds to thousands of times. We determined the optical density of each well at 450 nm. The results were analyzed using EPOCH Gen 5 software. We calculate the spike protein levels in a dose with a standard curve.

Experimental method

To evaluate the efficacy and safety of the prepared vaccine, 50-60 days old, 20 female Balb/c mice were randomly divided into 6 groups. Animals were kept in IVC cages (22°C, 55-65 % relative humidity), all groups were separated, they were fed with ad libitum and animals had access to food and water whenever they wanted. Group N1 animals received virus only (n = 2), group N2 received no application (n = 2), group G1 received virus and 1 µg intraperitoneal vaccine (n = 4), group G2 received virus and 6 µg intraperitoneal vaccine (n = 4), group G3 received virus and 10 µl intraperitoneal vaccine (n = 5), group G4 received 4 µl vaccine only (n = 2). The vaccine was administered on days 0 and 21. On day 35, N1, G1, G2, and G3 received intranasally 10^4 $TCID_{50}$ live viruses Sars-CoV-2, which was administered into both nasal passages using a micropipette in an isolator (220 Pa negative pressure). All animals were sacrificed on day 45.

Animals were subjected to routine necropsy, organ tissue samples were collected in 10% formalin solution and subjected to routine tissue examination and embedded in paraffin blocks. Sections 3-4 µm thick were collected from each block using a rotary microtome (Leica RM2255,Germany), stained with hematoxylin & eosin (H&E), and analyzed under a light microscope (Olympus BX50, Japan). All histopathological examinations were double-blinded and scored by each pathologist and their mathematical mean was accepted as the true value.

Results

Vaccine preparation

Microcarrier-based production in disposable wave bioreactors (SARTORIUS Biostat RM20, Germany) was very efficient for vaccine production. Disposable bags are easily maintained, and aseptic connections of bags are very useful for dangerous pathogens. Cells are growing very fast and healthy in appropriate conditions (rocking, pH, angle and, gases control). All manipulations are carried out aseptically and safely. However, 0.05 MOI was found optimal multiply of infection ratio to infect VERO CCL-81 cells.

ELISA

We found the SARS-COV-2 Spike protein quantity is equal to 7.53 ng/ml in 1:75 dilution of the main bulk of the vaccine candidate. Each dose of the vaccine candidate contains about 340 –400 ng viral spike protein (Table 1).

Table 1
SARS-COV-2 Spike protein quantities

Sample and Standarts	Absorbance	Concentration pg/ml
STD 1 10000 pg/ml	2,896	10840,095
STD 2 5000 pg/ml	1,645	5486,138
STD 3 2500 pg/ml	0,853	2486,339
STD 4 1250 pg/ml	0,406	1014,814
STD 5 625 pg/ml	0,246	554,92
STD 6 312,5 pg/ml	0,145	293,464
STD 7 156,25 pg/ml	0,103	195,136
Negative	0,078	139,697
Main bulk 1/75 dilutıon	2,14	7529,486

Virus titration

Virus titration P3 master seed lot was reaching a peak titer over $1.3x10^7$ PFU by 72 - 76 h post-infection (hpi) at multiplicities of infection (MOI) of 0.01. Growth kinetic analysis of the P5 stock in Vero cells showed that the stock virus could replicate efficiently and reached a peak titer 1.6×10^7 PFU by 56–72 h post-infection (hpi) at multiplicities of infection (MOI) 0.05 (Figure 3).

Inactivation validation

No CPE was observed for three passages Inactivation was validated by passaging the treated samples 3 generations (n=3) without the appearance of CPE [8]. Double BPL inactivation provides a rapid and safe method for the inactivation of viral particles.

Quantitative RT- PCR

Genesig/Primerdesign qRT-PCR kit results are compatible with viral titer results at 52 – 76 h. Later, viral load was increasing, but the viral titer decreased due to the virus viability. It's a fast way to the determination of harvesting time. However, the preparation of viral stocks' viral titers should be determined before and after the storage in liquid nitrogen.

Sequencing

Sequence distance matrix of first, third and, ninth passages of SARS-COV-2 in VERO Cell culture. All these passages correlate to SARS-COV-2 NC 045512 isolate at a ratio of 97.891 to 99.117 % in the NCBI database. It was determined that the 1 st passage, 4th passage, and 9th passage of SARS-CoV-2 genome sequences matched 100 %, and all the mutations in the first sample were also observed completely in the other samples. Some negligible deletions were observed in the sequences, not in the affected structure of the virus. The variations were found to correspond to the genomic positions 313, 5554, 8782, and 17259 (ORF1ab gene), 21784 and 22468 (S gene), 28878 (N gene), 28144 (ORF 8 gene), 26873 (M gene), and 29742 (3’ UTR).

Western blot and SDS page

It is observed that Spike, Nucleoprotein and, Membran proteins are approximately 190, 48, 26 kDa, respectively after the purification step (Figure 5). SARS-CoVN and SARS-CoVS proteins are determined by incubation with anti-SARS-COV-2 N, S antibodies and, HRP conjugated rabbit antibodies in Western Blot.

TEM

TEM analysis verified the viral replication in VERO cells and showed intact, oval-shaped particles with diameters of 90 to 110 nm of the virus after the final purification step (Figure 6).

Vaccine immunogenicity analysis and neutralization assay

The preliminary results in mice showed that the NtAb titers reached the peak post-priming and boosting in 21 days. The titers were respectively 1/ 595, 1 /791, and 1/1048 in 4, 6, and 10 µg groups (Figure 7).

Macroscopic Findings

Although there were no significant differences between the groups in the macroscopic examination, depending on the euthanasia method applied (decapitation), bleeding areas were observed in the head, neck, and back regions, and in some animals, blood accumulation/collections in the lungs due to blood aspiration were observed.

Histopathology Findings:

Histopathologic changes observed in animals are given in Table 2. In the histopathologic evaluation, the main differences between groups were observed especially in the lung, heart, abdominal lipid tissue, and spleen.

Table 2
Histopathologic changes observed in animals

Tissue	Histopathology	N1 (CoV)		N2		G1 (CoV+1µl vaccine)					G2 (CoV+6µl vaccine)				G3 (CoV+10µl vaccine)			
		1	2	1	2	1	2	3	4	5	1	2	3	4	1	2	3	4
Lung	Perivascular lymphoid infiltration	+	++	-	-	++	++	++	-	++	-	-	++	++	+		+	+
	Peribronchial lymphoid infiltration	-	++	-	-	++	++	++	-	++	-	-	+++	++	++	++	+	+
	Bronchial epithelial hyperplasia/hypertrophia	-	-	-	-	-	-	-	-	-	-	-	-	-	-	+	-	+
	Hemorrhage	+ (local)	-	-	-	++	-	-	-	++	-	-	++	-	+	-	-	-
	Emphysema	+	+	-	-	+	-	-	-	-	-	-	-	++	+	+	+	+
	Alveolar macrophage infiltrations	-	+	-	-	-	+	-	-	+	-	-	++	-	-	-	-	+
	Intraalveolaer mononuclear cells infiltrations	-	+	-	-	-	-	-	-	+	-	-	+++	-	-	-	-	+
	İntraalveolar polymorph cell infiltration	-	+	-	-	-	-	-	-	-	-	-	-	-	-	-	-	-
	Interstitial pneumonia	-	++	-	-	-	-	-	-	-	-	-	-	-	-	-	-	-
	Fibrinoid necrosis in small vessels	-	++	-	-	+	+	-	++	-	-	-	++	-	-	-	-	-
	Per diapedesis hemorrhage	-	+	-	-	-	-	-	++	-	+	-	-	-	-	-	-	-
	Fibrin inside the alveoli	-	-	-	-	-	-	-	+	-	-	-	-	-	-	-	-	-
	Thrombosis	-	-	-	-	-	-	-	-	++	-	-	-	-	-	+	-	-
	Tumor	-	-	++	-	-	-	-	-	-	-	-	-	-	-	-	-	-
	Hyperemia	-	-	-	-	-	++	-	++	-	++	-	++	++	+	-	-	+
	Bronchiectasis	-	-	-	-	-	-	-	-	-	-	++	-	-	-	-	-	-
	Hyaline accumulation in the bronchus	-	+	-	-	-	-	-	-	-	-	-	-	-	-	-	-	-
CNS	Meningeal lymphoid infiltration	+	-	-	-	-	-	-	-	-	-	+	-	+	-	-	-	-
	Micro thrombosis	-	-	-	-	-	-	-	-	-	-	-	+	-	-	-	-	-
	Hemorrhage	-	-	-	-	-	-	-	-	-	-	-	+	-	-	-	-	-
	Perivascular lymphoid infiltrations	-	-	–	-	-	-	-	-	-	-	-	++	-	-	-	-	-
Heart	Zenker degeneration/necrosis	+	++	-	-	-	+	++	-	+	++	+++	+++	-	++	+	+	+
	Mononuclear cell infiltration	-	+	-	-	-	-	-	-	-	-	-	-	-	-	-	-	-
	Hemorrhage	-	-	-	-	-	-	-	-	-	+	-	-	-	-	-	-	-
Abdominal lipid tissue	Lymphoid infiltration	-	-	-	-	+++	++	-	-	+	+++	-	-	+++	+	++	++	-
	Abdominal fat necrosis	-	-	-	-	-	-	-	-	-	-	-	-	+++	-	-	+	-
	Granuloma	-	-	-	-	-	-	-	-	-	-	-	-	-	+	++	+++	+
Liver	Parenchymatous degeneration	+++	+++	++	++	+++	++	+	+++	+++	+	++	+++	++	++	+++	+++	+
	Fatty degeneration	-	-	+	+	+	+	-	-	+	-	+	+	+	+	++	+	+
	Hepatitis	++	-	-	-	-	-	-	-	-	-	-	-	-	-	-	-	-
	Hemorrhage	++	-	-	-	-	-	-	-	-	-	-	-	-	-	-	-	-

Spleen	Lymphoid hyperplasia	+	++	-	-	+	++	+	++	++	++	+++	-	++	++	++	+++	+
	Increased megakaryocytes	-	-	-	-	-	-	-	-	-	-	-	-	-	++	+	++	+
	Congestion	-	-	-	-	-	-	-	-	-	-	-	-	-	+	+	+++	+
Kidney	İnterstitial nephritis	-	-	-	-	-	-	-	-	-	-	-	-	-	+	-	-	+
	Hyperemia	-	-	-	-	-	-	-	-	-	-	-	-	-	+	++	+	+

In the lungs, the most significant findings were the perivascular and peribronchial mononuclear cell infiltrates, especially in animals that received vaccination and they were more prominent in the 6 and 10 µl vaccine groups (Figure 8A, 8B). And only in G3 bronchial epithelial hyperplasia/hypertrophia is observed. Hemorrhages were observed in all groups in which we assumed blood aspiration due to the decapitation process. Interstitial pneumonia is only observed in one animal (N2) which only received a virus. Thrombosis in small vessels and inside alveoli and hyaline accumulation inside alveoli were observed especially in G4 in animals (Figure 8C, 8D) only received 4 µl vaccination.

In the central nervous system, some meningeal lymphoid infiltrations and per diapedesis bleeding were observed in 5 animals; N1-1, G2-1, G2-4, G3-5, and G4-1(Figure 8E), and hemorrhage, micro thrombosis, and perivascular lymphoid infiltrations are observed only in G2-3 (Figure 8F).

Varying degrees of hemorrhages, myofiber degenerative changes (Zenker degenerations), and necrosis, mononuclear cell infiltrations were detected in the heart (Figure 8G). Only the animals in the group that did not receive any treatment or virus application (N2) heart tissues were healthy. The degenerative changes were distinct, especially in G2 (Figure 8H) and they are generally located on the left side of the heart.

Widespread parenchymatous degeneration and varying degrees of fatty degeneration were detected in the livers of all animal groups. Only hepatitis and hemorrhages were observed in one animal (N1).

In all groups which received intraperitoneal vaccination varying degrees of changes were observed in the abdominal lipid tissue. G3 animals which received 10 µl intraperitoneal vaccination demonstrated the severest cases. Lymphocytic infiltrations, macrophages, necrosis, granulomatous changes, and granulomas are observed (Figure 8I). In one animal (G2-4) where these changes were close to the pancreatic tissue, degenerative changes and lymphocytic infiltrations were observed in the pancreatic tissue.

In the splenic tissue of animals, lymphocytic hyperplasia was significant in all groups with vaccinations (Figure 8J). Increased megakaryocytes in the spleen are observed in all animals.

In kidneys, hyperemia and interstitial nephritis were only observed in groups G3 and G4, and small degrees of lymphocytic infiltration especially in the renal pelvis were determined.

Discussion

In the development of the vaccine candidate, the candidate strain generated the highest virus yields in Vero cells CCL-81 and had no amino acid variations within 9 passages, suggesting its good genetic stability. We observed only some deletions in the full genome sequence but not affected the amino acid structure of the basic structure of the virus. Pavel et. al. [13] found the variations that genomic positions 1397 and 11083 (ORF1ab gene), 23876 (S gene), 26688 (NP gene), 29563 (ORF 10 gene), and 29742 (3' UTR). Also, Gao et al. [6] reported that some genetic alterations between in the passaging levels of virus, but not affecting to immunity. In this study, we found the variations that genomic positions 313, 5554, 8782 and 17259 (ORF1ab gene), 21784 and 22468 (S gene), 28878 (N gene), 28144 (ORF 8 gene), 26873 (M gene), and 29742 (3' UTR). These differences may be affected immunity to wild-type virus strains slightly, but it will become clear after the cohort studies to be carried out on large scale.

Due to high viral yield, microcarrier size and concentration, Vero cell seeding quantity, multiply of infection ratio, time and duration of viral infection, maintenance of pO2, pH, bioreactor angle and shaking, and time of harvesting are critical factors in the upstream process. The pO2 saturation must not be decreased below 35 % and pH should be maintained around 7 to avoid the aggregation and lyses of viral proteins and supported cell growth and viral production. 56 – 72 h was found optimal harvesting time in these production conditions. Our data is in agreement with a study of Manenti et al. [10] in which SARS-CoV-2 replicated rapidly in Vero CCL-81 cells after an initial eclipse phase and increased gradually, peaking at 56 h post-infection.

However, the latest report shows in the preparation of vaccines, Double BPL inactivation provides a rapid and safe method for the inactivation of viral particles [15]. Also, intact viral particles are apparent by transmissible electron microscopy (TEM). In TEM analysis showed intact, oval-shaped particles with diameters of 90 to 110 nm of the virus after the final purification step. Our data is in agreement with that of Jureka et. al. [8], in which TEM analysis showed 90 -110 nm virus in purified bulk.

Quantitative SARS-CoV-2 Spike antigen ELISA test verified SDS gel antigen quantities with working BSA standards in SDS gel electrophoresis. Also, quantitative RT-PCR results from the Genesig COVID-19 RT-PCR kit gave information about the viral titers and viral protein quantity with invert microscopy examination to decide harvesting time of viral bulk.

We demonstrated that both nucleoprotein and spike (full-length and cleaved) of SARS-CoV-2 in all downstream process steps are detectable by western blot in these samples.

The two-dose immunizations with median doses (4 µg, 6 µg, and 10 µg) at days 0/21, found efficient in K18 hACE-2 transgenic mice challenge studies (data not shown). SARS COV-2 vaccine candidate induces high levels of Nab titers and efficiently protects them in suitable animal models (Balb/c and K18 hACE-2 mice).

We used the ANOVA method to compare the log-transformed antibody titer depends on the normality test results that showed normal distribution. When the comparison among all five groups showed a significant difference between vaccinated and non-vaccinated (Placebo) groups, we then did pair-wise comparisons. Median doses (4 and 6 µg) showed a good immune response and not any gross and pathological findings.

SARS CoV-2 vaccine candidate is efficiently produced, genetically stable, and safe in Balb/c mice, hACE-2 transgenic mice, and transgenic ferrets (data not shown). Clinical evaluations included temperature, weight loss, fever, dyspnoea, lethargy, anorexia, and grooming. In transgenic ferrets, the deactivated vaccine doses were well tolerated in all dose groups with no vaccine-related serious adverse effects. The most common adverse reaction was injection site swelling, which was mild and limited. Fever, inappetence, and weight loss were not observed in Balb/c mice and transgenic ferrets [1, 16].

During the study, no differences in body weight, body temperature, or clinical pathology were observed or detected in ferrets and mice inoculated with the lowest and highest doses of the vaccine candidate, compared with control groups [1, 6].

No obvious systemic toxicity was observed in any animal species during the dosing period and at the end of the 2-week recovery period. Local skin irritation reactions related to alum adjuvants were noted on injection sites, but they disappeared within a week [6].

The results showed that the vaccine candidate stimulated immoral immune responses and presented no toxicity in animals tested. In conclusion, a study on the safety and immunogenicity of the inactivated, whole virus vaccine showed the vaccine stimulated a strong humoral immune response. In this study, the preliminary results in mice showed that the NtAb titers reached the peak post-priming and boosting in 21 days. Titers in 4, 6, and 10 µg groups found about 1/595, 1/791, and 1/1048, respectively. The mice have been injected twice at doses of 4 µg and 6 µg/mouse 21 days interval and NtAb levels remain high for 6 months (Unpublished data).

Even the placebo and vaccination of Balb/c mice were challenged with 10^5 TCID50 doses of SARS-CoV-2 by the intranasal route, lethality and clinical pneumonia were not reported. SARS-CoV–2 showed good binding for human ACE2 but limited binding to mice ACE2. The SARS-CoV-2 virus showed slight pneumonia without apparent clinical signs and replication was remained in limit in other epithelial tissues [6].

Based on the results presented here, a Phase I clinical trial of candidate COVID-19 vaccine is currently in progress and a Phase II of the clinical trial has recently been initiated. These clinical trials have been designed using the same aluminum adjuvant formulation described here, with two different groups of 4, and 6 µg dose groups to evaluate the appropriate dose for further clinical application.

About the histopathologic examination of the organs on Balc/c mice, there were not any reports we found that performs systemic examinations. The published report generally investigates changes in lung tissue and olfactoric bulbs in Balb/c mice [1, 17].

In all groups that received intraperitoneal vaccination, varying degrees of changes were observed in the abdominal lipid tissue. These findings were similar to the findings of Portuondo et. al. [18] where they observed palpable nodules at the injection site in all animals injected with aluminum hydroxide adjuvants. Meningeal lymphoid infiltrations observed in animals were similar in cases in humans with focal leptomeningeal inflammation described by Lee et. al. [19]. However, we could not detect any reports regarding the changes observed in Balb/c mice. The most significant finding was varying degrees of hemorrhages and Zenker degenerations in the heart of animals that receive treatment and/or virus application. These changes were similar to the findings reported in Syrian hamsters [16, 20] and humans [21]. The findings of mild focal myocardial degeneration in Syrian hamsters after virus application were similar to our findings and observed more intensely in non-vaccinated animals than vaccinated animals. Widespread parenchymatous degeneration and varying degrees of fatty degeneration were detected in the livers of all animal groups. Detecting these changes in all animals gives rise to the thought of changes due to ad libitum feeding, type of feed, or inactivity inside the cages. The changes observed in the kidneys were limited to 2 animals from different groups, and due to small populations, we thought they could be negligible and no literature data in Balb/c to compare was determined.

In the literature about Balb/c mice generally, lung tissue changes were observed in aged mice [1, 17, 22]. When the necropsies were performed our mouse population was aged between 90-100 days. According to Hongjing et. al. [1] modified virus applications similar to our modification can cause some changes in the young Balb/c mouse at early ages, and this finding was like our findings in the lung tissues. The increased lymphocytic infiltration especially in the vaccinated group was thought to be due to the immune response gained by the vaccine. Small doses of vaccination were observed to cause vascular changes but to report that much larger populations, where statistical analyzes can be performed should be used. Like in the lung tissue increased lymphocytic hyperplasia in the splenic tissue of vaccinated animals was thought to be due to the immune response gained by the vaccine. Increased megakaryocytes in the spleen are observed in all animals which we think is a result of repetitive blood collections for titrations.

Conclusion

In the presented study the preclinical development of an inactivated COVID-19 vaccine candidate is described. Initial results describing the immunogenicity of the COVID-19 vaccine candidate, are promising, and it is particularly encouraging to measure neutralization antibodies and cellular responses in Balb/c mice. We provide evidence for the safety of inactivated COVID-19 vaccine candidates in Balb/c mice and did not observe infection enhancement and immunopathological changes in two doses vaccinated Balb/c mice.

Abbreviations

- SARS-CoV-2: Severe Acute Respiratory Syndrome Coronavirus 2

- MERS-CoV: Middle East Respiratory Syndrome Coronavirus

- qRT-PCR: Quantitative Real Time Polymerase Chain Reaction

- TEM: Transmissible Electron Microscopy

- BPL : Beta-propiolacton

- CPE : Cytopathic Effect

- TCID: Tissue Culture Infected Dose

- hACE-2: Human Acetylcholine esterase 2

Declarations

Ethics declarations

The Animal Local Ethics Committee of Kocak Pharmaceuticals approved all animal experiment in this study (No. 2020-5).

Availability of data and material

The key information and data generated and/or analyzed during this study were included in this article.

Human tissue, human participants and human data

Not applicable.

Consent for publication

Not applicable.

Competing interests

The authors declare no conflict of interest.

Acknowledgments

Not applicable.

Funding

Engin Alp ONEN reports financial support was provided by Kocak Farma Pharmaceutical Company.

Contributions

Individual contributions to the work are as follows: Conception and study design, EAO, EAO; data acquisition and analysis, EAO, EKD, KS; drafting of the manuscript, KS, FY; translation and editing of the manuscript, EAO,KS, FY, AG, and critical revision of the manuscript, EAO,KS, FY, AG. All authors read and approved the final manuscript.

References

1. Gu H, Chen Q, Yang G, He L, Fan H, Deng YQ, Wang Y, Teng Y, Zhao Z, Cui Y, Li Y, Li XF, Li J, Zhang NN, Yang X, Chen S, Guo Y, Zhao G, Wang X, Luo DY, Wang H, Yang X, Li Y, Han G, He Y, Zhou X, Geng S, Sheng X, Jiang S, Sun S, Qin CF, Zhou Y. Adaptation of SARS-CoV-2 in BALB/c mice for testing vaccine efficacy. Science. 2020 Sep 25;369(6511):1603-1607. doi: 10.1126/science.abc4730. Epub 2020 Jul 30. PMID: 32732280; PMCID: PMC7574913.
2. Tang X, Wu C, Li X, Song Y, Yao X, Wu X, et al. On the origin and continuing evolution of SARS-CoV-2. Natl Sci Rev 2020;7. https://doi.org/10.1093/nsr/nwaa036.
3. Lu R, Zhao X, Li J, Niu P, Yang B, Wu H, et al. Genomic characterisation and epidemiology of 2019 novel coronavirus: implications for virus origins and receptor binding. Lancet 2020;395. https://doi.org/10.1016/S0140-6736(20)30251-8.
4. Andersen KG, Rambaut A, Lipkin WI, Holmes EC, Garry RF. The proximal origin of SARS-CoV-2. Nat Med 2020;26. https://doi.org/10.1038/s41591-020-0820-9.
5. Spruth M, Kistner O, Savidis-Dacho H, Hitter E, Crowe B, Gerencer M, et al. A double-inactivated whole virus candidate SARS coronavirus vaccine stimulates neutralising and protective antibody responses. Vaccine 2006;24. https://doi.org/10.1016/j.vaccine.2005.08.055.
6. Gao Q, Bao L, Mao H, Wang L, Xu K, Yang M, Li Y, Zhu L, Wang N, Lv Z, Gao H, Ge X, Kan B, Hu Y, Liu J, Cai F, Jiang D, Yin Y, Qin C, Li J, Gong X, Lou X, Shi W, Wu D, Zhang H, Zhu L, Deng W, Li Y, Lu J, Li C, Wang X, Yin W, Zhang Y, Qin C. Development of an inactivated vaccine candidate for SARS-CoV-2.

Science. 2020 Jul 3;369(6499):77-81. doi: 10.1126/science.abc1932. Epub 2020 May 6. PMID: 32376603; PMCID: PMC7202686.

7. Wang H, Zhang Y, Huang B, Deng W, Quan Y, Wang W, et al. Development of an Inactivated Vaccine Candidate, BBIBP-CorV, with Potent Protection against SARS-CoV-2. Cell 2020;182. https://doi.org/10.1016/j.cell.2020.06.008.
8. Jureka A, Silvas J, Basler C. Propagation, Inactivation, and Safety Testing of SARS-CoV-2. Viruses 2020;12. https://doi.org/10.3390/v12060622.
9. Kärber G. Beitrag zur kollektiven Behandlung pharmakologischer Reihenversuche. Naunyn Schmiedebergs Arch Exp Pathol Pharmakol 1931;162. https://doi.org/10.1007/BF01863914.
10. Manenti A, Maggetti M, Casa E, Martinuzzi D, Torelli A, Trombetta CM, et al. Evaluation of SARS-CoV-2 neutralizing antibodies using a CPE-based colorimetric live virus micro-neutralization assay in human serum samples. J Med Virol 2020;92. https://doi.org/10.1002/jmv.25986.
11. Tan CW, Chia WN, Qin X, Liu P, Chen MI-C, Tiu C, et al. A SARS-CoV-2 surrogate virus neutralization test based on antibody-mediated blockage of ACE2–spike protein–protein interaction. Nat Biotechnol 2020;38. https://doi.org/10.1038/s41587-020-0631-z.
12. Muruato AE, Fontes-Garfias CR, Ren P, Garcia-Blanco MA, Menachery VD, Xie X, et al. A high-throughput neutralizing antibody assay for COVID-19 diagnosis and vaccine evaluation. Nat Commun 2020;11. https://doi.org/10.1038/s41467-020-17892-0.
13. Pavel STI, Yetiskin H, Aydin G, Holyavkin C, Uygut MA, Dursun ZB, et al. Isolation and characterization of severe acute respiratory syndrome coronavirus 2 in Turkey. PLoS One 2020;15. https://doi.org/10.1371/journal.pone.0238614.
14. Lu X, Wang L, Sakthivel SK, Whitaker B, Murray J, Kamili S, et al. US CDC Real-Time Reverse Transcription PCR Panel for Detection of Severe Acute Respiratory Syndrome Coronavirus 2. Emerg Infect Dis 2020;26. https://doi.org/10.3201/eid2608.201246.
15. Xia S, Duan K, Zhang Y, Zhao D, Zhang H, Xie Z, et al. Effect of an Inactivated Vaccine Against SARS-CoV-2 on Safety and Immunogenicity Outcomes. JAMA 2020;324. https://doi.org/10.1001/jama.2020.15543.
16. Zeiss CJ, Compton S, Veenhuis RT. Animal Models of COVID-19. I. Comparative Virology and Disease Pathogenesis. ILAR J 2021. https://doi.org/10.1093/ilar/ilab007.
17. Dinnon KH, Leist SR, Schäfer A, Edwards CE, Martinez DR, Montgomery SA, et al. A mouse-adapted model of SARS-CoV-2 to test COVID-19 countermeasures. Nature 2020;586:560–6. https://doi.org/10.1038/s41586-020-2708-8.
18. Portuondo DL, Batista-Duharte A, Ferreira LS, de Andrade CR, Quinello C, Téllez-Martínez D, et al. Comparative efficacy and toxicity of two vaccine candidates against Sporothrix schenckii using either Montanide™ Pet Gel A or aluminum hydroxide adjuvants in mice. Vaccine 2017;35. https://doi.org/10.1016/j.vaccine.2017.05.046.
19. Lee MH, Perl DP, Nair G, Li W, Maric D, Murray H, Dodd SJ, Koretsky AP, Watts JA, Cheung V, Masliah E, Horkayne-Szakaly I, Jones R, Stram MN, Moncur J, Hefti M, Folkerth RD, Nath A. Microvascular Injury in the Brains of Patients with Covid-19. N Engl J Med. 2021 Feb 4;384(5):481-483. doi: 10.1056/NEJMc2033369. Epub 2020 Dec 30. PMID: 33378608; PMCID: PMC7787217.
20. Chan JF-W, Zhang AJ, Yuan S, Poon VK-M, Chan CC-S, Lee AC-Y, et al. Simulation of the Clinical and Pathological Manifestations of Coronavirus Disease 2019 (COVID-19) in a Golden Syrian Hamster Model: Implications for Disease Pathogenesis and Transmissibility. Clin Infect Dis 2020. https://doi.org/10.1093/cid/ciaa325.
21. Diaz GA, Parsons GT, Gering SK, Meier AR, Hutchinson I V., Robicsek A. Myocarditis and Pericarditis After Vaccination for COVID-19. JAMA 2021. https://doi.org/10.1001/jama.2021.13443.
22. Zhang Y, Huang K, Wang T, Deng F, Gong W, Hui X, et al. SARS-CoV-2 Rapidly Adapts in Aged BALB/c Mice and Induces Typical Pneumonia. J Virol 2021;95. https://doi.org/10.1128/jvi.02477-20.

Figures

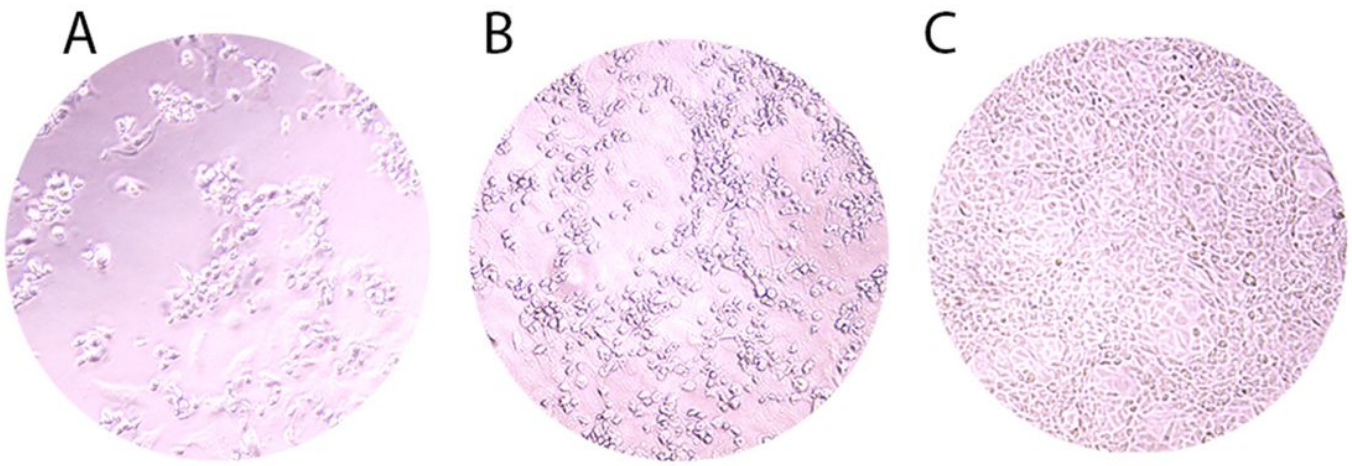

Figure 1

Vero CCL-81 cells at different stages of infection. A. SARS-CoV-2 infected VERO CCL-81 cell monolayer after 48 hours postinfection, 80 - 90 % of CPE recovered B. SARS-CoV-2 infected VERO CCL-81 cell monolayer after 62 hours postinfection, 30 % -40 % of CPE recovered. C. Not infected VERO CCL-81 cell monolayer after 62 hours, complete absence of CPE.

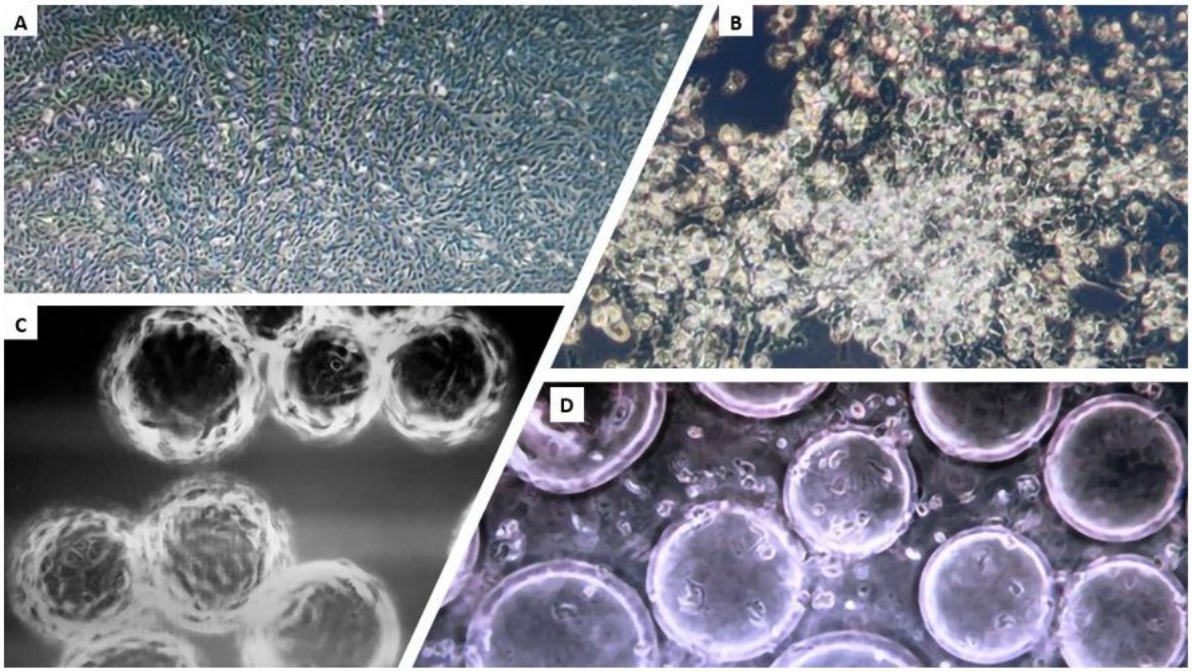

Figure 2

Propagation of SARS-CoV-2 in VERO CCL-81 cell culture. A. Healthy and confluent VERO cells in T-Flasks. B. 72.h after the inoculation of SARS-CoV-2 in T-Flasks. C. Healthy and confluent VERO cells on Cytodex-1 microcarriers in Biostat RM 20L Bioreactor. D. 72 – 96 .h after the inoculation of SARS-CoV-2 on Cytodex-1 microcarriers in Biostat RM 20L Bioreactor.

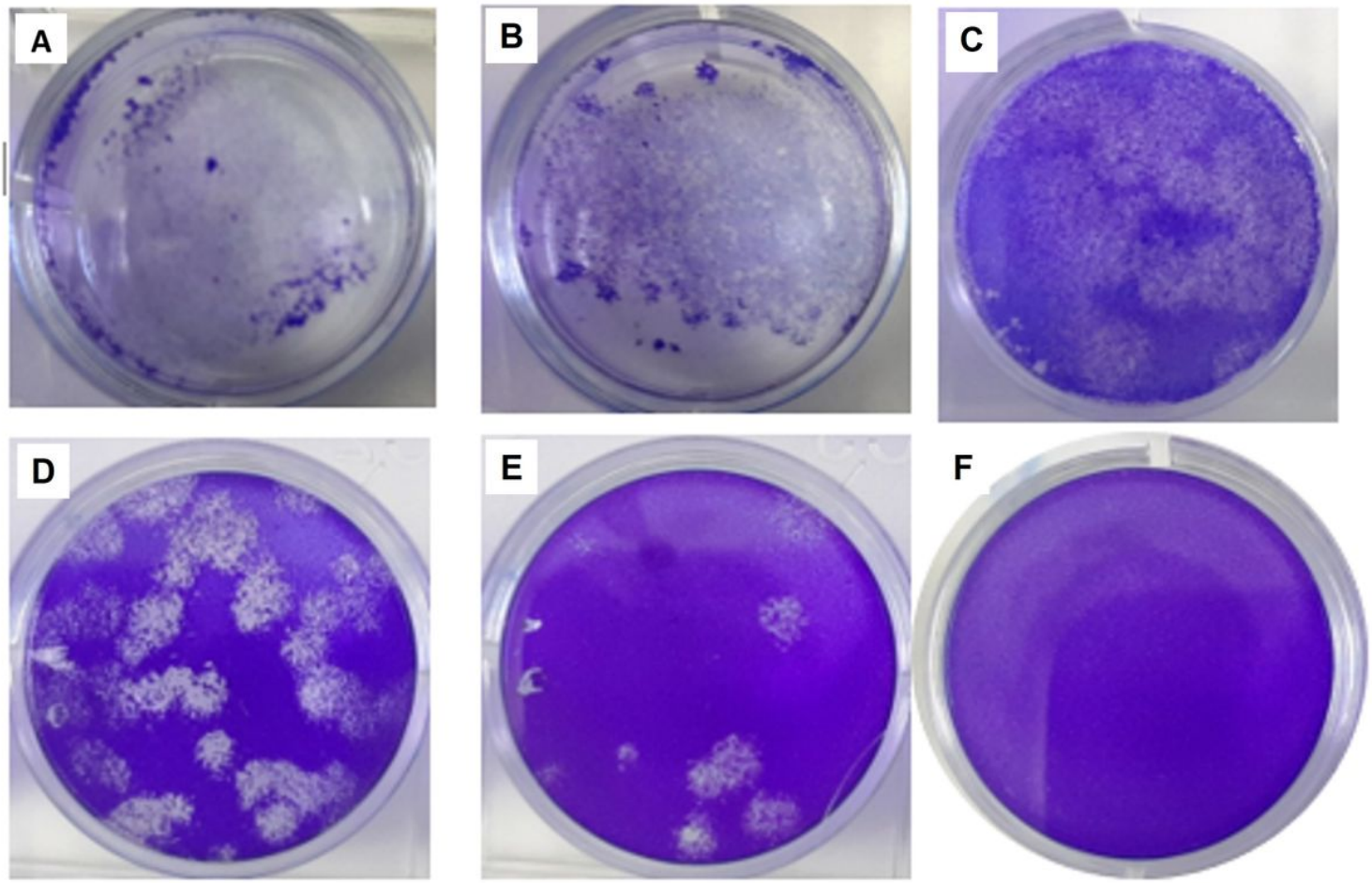

Figure 3

Quantification of SARS-CoV-2 in CCL-81 cell culture. Plaque assays were harvested at 72 h post-infection, fixed, and stained with crystal violet to visualize. A, B, C, D, E wells are ten-fold dilutions of virus and F well is the negative control.

Basic Relative Quantification for All Samples (Relative Quantification)

Abs Quant/Fit Points for nCOV-2 22.08.20 (Abs Quant/Fit Points)

Settings

Channel	465-510				
Color Compensation	Off				
Standard Curve	Set Efficiency (2.00)				
Program	Amplification			Units	
First Cycle	1	Last Cycle	45	Background	2-6
Noiseband Method	STD Mult	Noiseband	1.1543	STD Dev Multiplier	12.0000
# of Fit Points	2	Threshold Method	Manual	Threshold	1.1543

Subset Name	nCOV-2 22.08.20

Results

Inc	Pos	Name	Type	CP	Concentration	Standard	Status
☑	B2	nCOV-2 P1 N1	Unknown	14.15			
☑	B4	nCOV-2 P1 N2	Unknown	13.72			
☑	B6	nCOV-2 P2 N1	Unknown	12.37			
☑	B8	nCOV-2 P2 N2	Unknown	12.60			
☑	B11	Negative	Negative Control				

Figure 4

qRT-PCR results for SARS-COV-2 passage 2 by cultivated in Vero CCL-81 cell line.

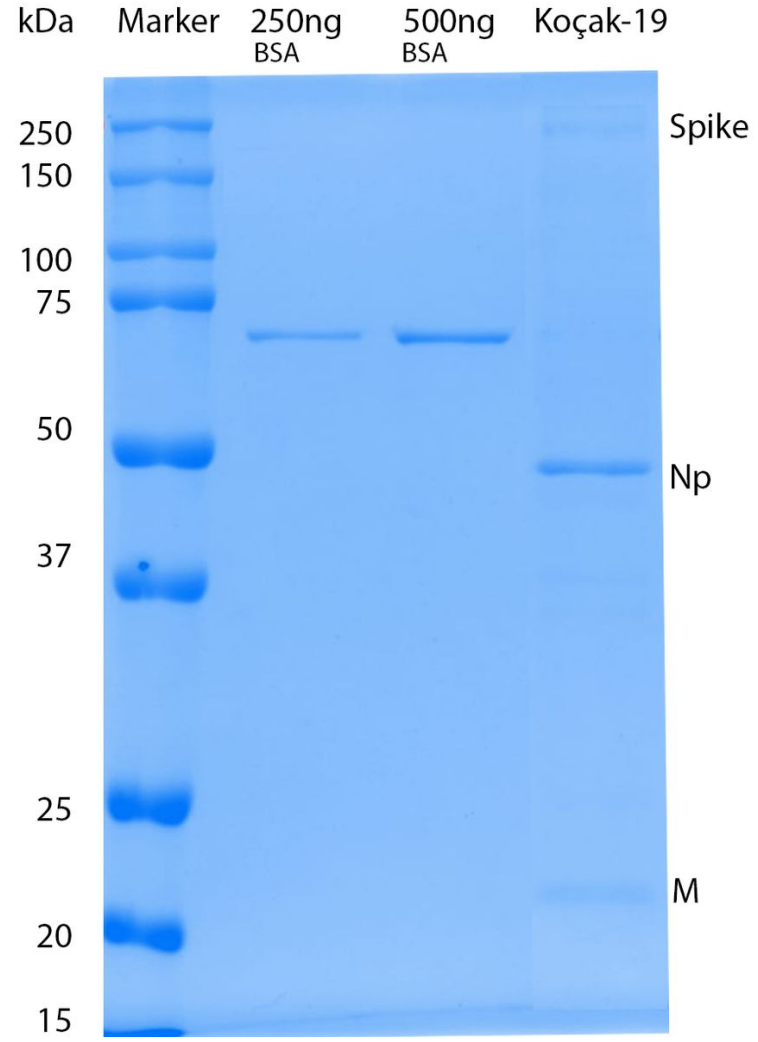

Figure 5

SARS-COV-2 SDS gel electrophoresis against known BSA standards.

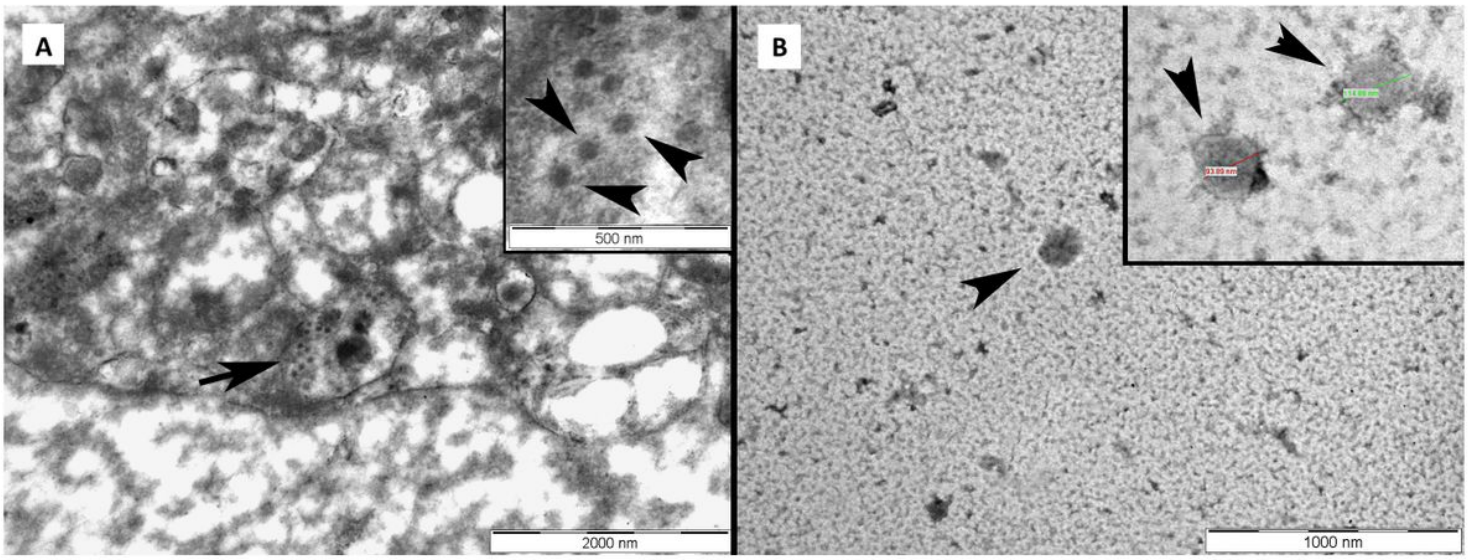

Figure 6

A. An infected VERO Cell containing a vesicle (arrow) filled with viral particles (arrow head). B. TEM images of oval-shaped particles with diameters of 90 to 110 nm of the virus (arrow head) after the final purification step.

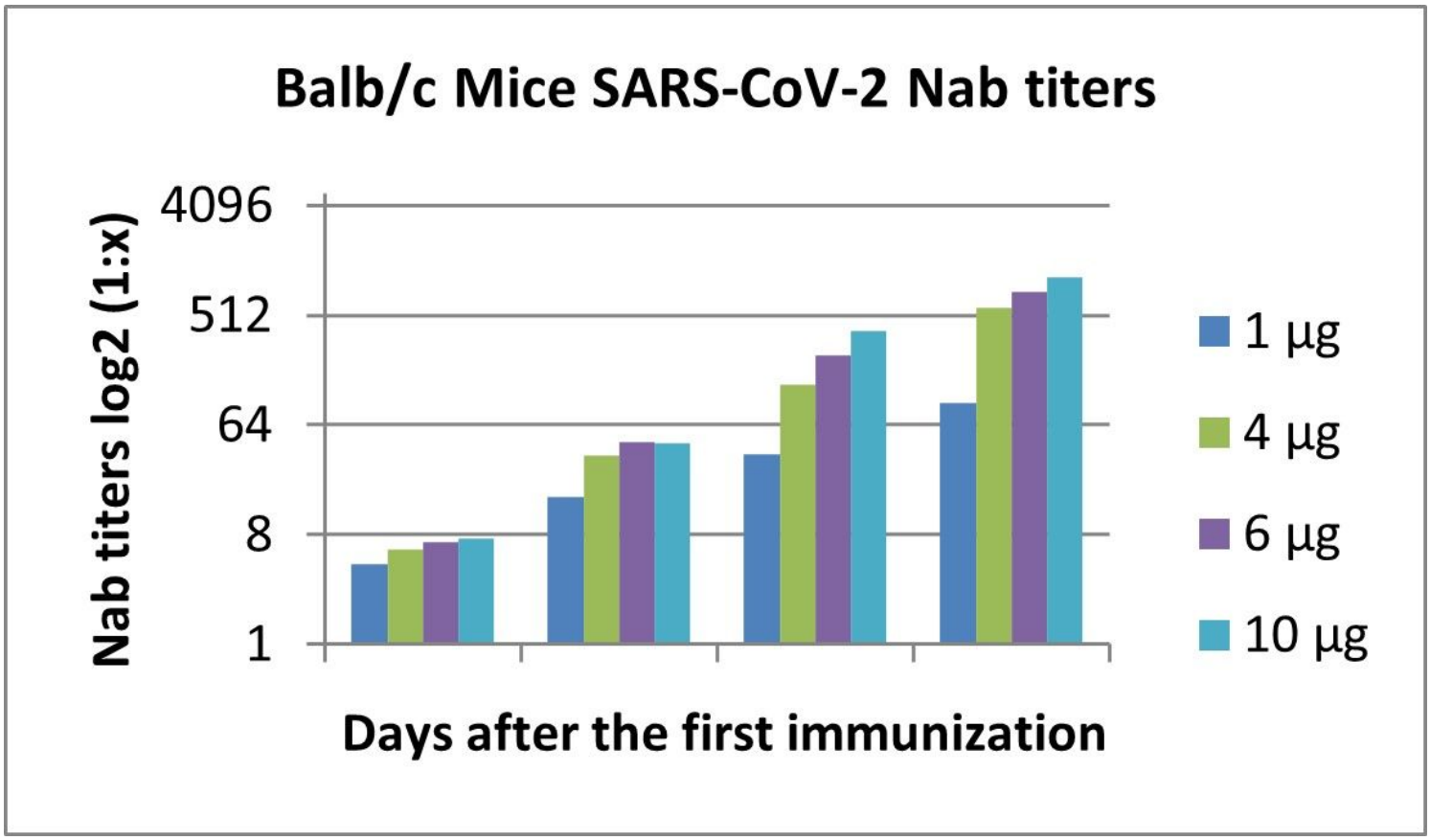

Figure 7

Mouse neutralization antibody (NAb) levels with different doses by two-dose immunization. Mice were injected intraperitoneally (IP) route by using two-time immunization (D0/D21), and the NAb levels at 14 days after the second immunization were tested by the microtitration method (n = 10).

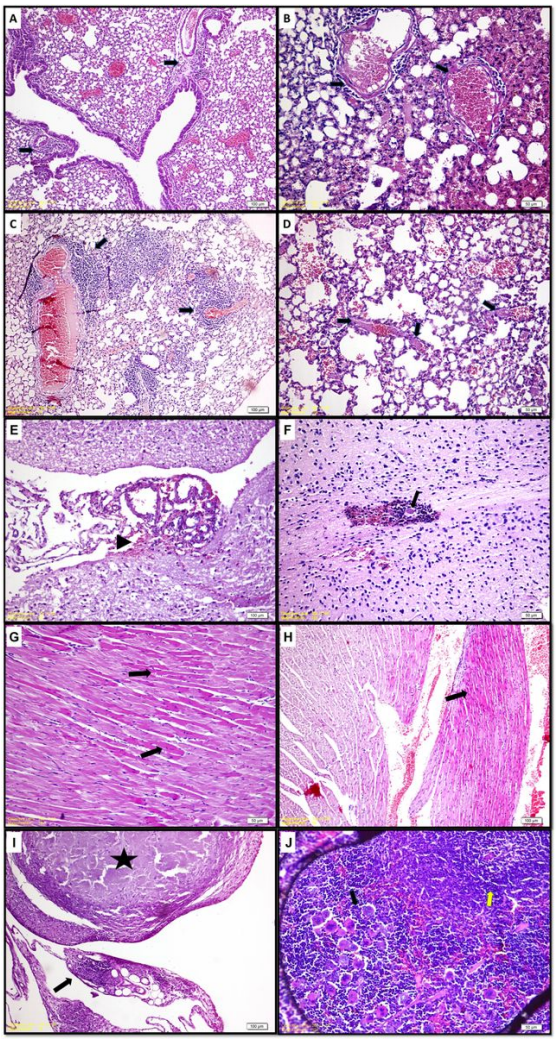

Figure 8

A) Changes in the lungs. Hematoxylin-eosin, G1-1, Perivascular and peribronchial lymphocytic infiltrations (arrow). B) Changes in the lungs. Hematoxylin-eosin, G1-4, Fibrinoid necrosis in the small vessels (arrow). C) Changes in the lungs. Hematoxylin-eosin, G2-3, Hyperemia, and perivascular lymphocytic infiltrations (arrow). D) Changes in the lungs. Hematoxylin-eosin, G4-2, Thrombosis in small vessels (arrow). E) Changes in the central nervous system. Hematoxylin-eosin, G2-4, Per diapedesis bleeding in the meninges (arrowhead). F) Changes in the central nervous system. Hematoxylin-eosin, G2-3, Perivascular lymphoid infiltrations, and micro thrombosis (arrow). G) Changes in the heart. Hematoxylin-eosin, G2-2, Widespread Zenker degenerations (arrow) H) Changes in the heart. Hematoxylin-eosin, G2-1, Widespread Zenker degenerations (arrow). I) Changes in the abdominal fat tissue. Hematoxylin-eosin, G4-4 Granulomatous changes; lymphocytic infiltrations, macrophages, and small necrosis (arrow). Wide calcified necrosis in a granuloma (star). J) Changes in the spleen. Hematoxylin-eosin, G2-2, Lymphocytic hyperplasia throughout spleen (yellow arrow) and increased megakaryocytes (black arrow).